Structural Fluctuations of a Cryptophane−Tetramethylammonium Host−Guest System: A Molecular Dynamics Simulation

Paul D. Kirchhoff,[†] Jean-Pierre Dutasta,[‡] André Collet,[‡] and J. Andrew McCammon*,[†]

Contribution from the Department of Chemistry and Biochemistry and Department of Pharmacology, University of California at San Diego, La Jolla, California 92093-0365, and Stéréochimie et Interactions moléculaires, École Normale Supérieure de Lyon, 46, allée d'Italie, F-69364 Lyon Cedex 07, France

Received April 14, 1997[⊗]

Abstract: Cryptophanes are aromatic hosts which bind a variety of guests. Here, we describe a 25 ns molecular dynamics simulation of a particular cryptophane host−guest complex in water. The cryptophane used in this study was used previously in a 20 ns molecular dynamics simulation to describe the fluctuations of the uncomplexed host. This cryptophane features three pores which open onto a cavity where the guests bind. In the current study, tetramethylammonium ion (TMA^+) has been placed within the cryptophane cavity to form the host−guest complex. The molecular dynamics simulation in combination with a surfacing algorithm provides information on the frequency with which the cryptophane pores open wide enough to admit or release guest molecules of any given size. We discuss these fluctuations and their possible consequences for binding kinetics, making comparisons between the cryptophane and the cryptophane−TMA^+ complex.

Introduction

Host−guest chemistry has attracted a great deal of attention for many years. It has practical importance in such areas as environmental remediation,[1,2] and fundamental importance in such areas as clarifying the principles of molecular recognition.[3−11] In this respect, there is a current interest for studies of the binding of quaternary ammonium cations (quats) to artificial receptors, in relation with the understanding of the complexation of acetylcholine and of related biomolecules to their natural receptors.[12−15]

Cryptophanes are a group of interesting cage-like host molecules that have been well-characterized in terms of the binding of guests of various sizes and net charges (including quats), in organic and aqueous solvents.[16−19] The cryptophane complexes are reversibly formed, and their stabilities (i.e., the magnitudes of their binding constants) depend on a variety of factors. Factors which do not directly involve the cryptophane, such as the solvent−guest interactions, may convey a significant contribution in the formation of cryptophane host−guest complexes. Even so, experimental data support the idea that host−guest and host−solvent interactions are dominant. For instance, it is likely that in aqueous solvents the host−solvent interactions will play a major role, because the cryptophane cavity is large enough to accommodate several water molecules, which would require displacement upon the binding of another guest.

Moreover, experiments indicate that the complexation and release of guest molecules is comparatively slow (barriers in the range of 10−17 kcal/mol), and static structures suggest that, for some guests, passage through a cryptophane pore is sterically hindered.[20] This implies that fluctuations of the pores may be important to the binding kinetics of guest molecules. In this study, molecular dynamics simulations have been conducted to obtain structural and conformational sampling information on a particular cryptophane-TMA^+ complex in water (TMA^+ = tetramethylammonium cation). The fluctuations of the cryptophane structure from the complex (and in particular of the pores and cavity) are characterized. Comparisons are made to a previous study involving the uncomplexed cryptophane, and the implications for the binding kinetics and stabilities are discussed.[21]

[†] University of California at San Diego.
[‡] École Normale Supérieure de Lyon
[⊗] Abstract published in *Advance ACS Abstracts,* August 1, 1997.

(1) Dang, L. X. *J. Am. Chem. Soc.* **1995**, *117*, 6954−6960.
(2) Schulz, W. W.; Bray, L. A. *Sep. Sci. Technol.* **1987**, *22*, 191−214.
(3) Marrone, T. J.; Merz, J. K. M. *J. Am. Chem. Soc.* **1992**, *114*, 7542−7549.
(4) Kearney, P. C.; Mizoue, L. S.; Kumpf, R. A.; Forman, J. E.; McCurdy, A.; Dougherty, D. A. *J. Am. Chem. Soc.* **1993**, *115*, 9907−9919.
(5) Axelsen, P. H. *Isr. J. Chem.* **1994**, *34*, 159−163.
(6) Marrone, T. J.; Merz, J. K. M. *J. Am. Chem. Soc.* **1995**, *117*, 779−791.
(7) Nakamura, K.; Houk, K. N. *J. Am. Chem. Soc.* **1995**, *117*, 1853−1854.
(8) Mordasini Denti, T. Z.; van Gunsteren, W. F.; Diederich, F. *J. Am. Chem. Soc.* **1996**, *118*, 6044−6051.
(9) Houk, K. N.; Nakamura, K.; Sheu, C.; Keating, A. E. *Science* **1996**, *273*, 627−629.
(10) Sheu, C.; Houk, K. N. *J. Am. Chem. Soc.* **1996**, *118*, 8056−8070.
(11) Fox, T.; Thomas, B. E., IV; McCarrick, M.; Kollman, P. A. *J. Phys. Chem.* **1996**, *100*, 10779−10783.
(12) Dougherty, D. A.; Stauffer, D. A. *Science* **1990**, *250*, 1558−1560.
(13) Méric, R.; Lehn, J.-M.; Vigneron, J.-P. *Bull. Soc. Chim. Fr.* **1994**, *131*, 579−583.
(14) Dougherty, D. A. *Science* **1996**, *271*, 163−168.
(15) Murayama, K.; Aoki, K. *J. Chem. Soc., Chem. Commun.* **1997**, 119−120.
(16) Canceill, J.; Cesario, M.; Collet, A.; Guilhem, J.; Lacombe, L.; Lozach, B.; Pascard, C. *Angew. Chem., Int. Ed. Engl.* **1989**, *28*, 1246−1248.
(17) Collet, A.; Dutasta, J.-P; Lozach, B.; Canceill, J. *Top. Curr. Chem.* **1993**, *165*, 103−129.
(18) Collet, A.; Dutasta, J.-P; Lozach, B. *Adv. Supramol. Chem.* **1993**, *3*, 1−35.
(19) Garel, L.; Vezin, H.; Dutasta, J.-P.; Collet, A. *J. Chem. Soc., Chem. Commun.* **1996**, *6*, 719−720.
(20) Collet, A. Cryptophanes. In *Comprehensive Supramolecular Chemistry*; Atwood, J. L., Davies, J. E. D., MacNicol, D. D., Vögtle, F., Eds.; Vol. 2, Ed. Vögtle, F.; Pergamon: New York, 1996, Chapter 11, pp 325−365.

S0002-7863(97)01186-4 CCC: $14.00

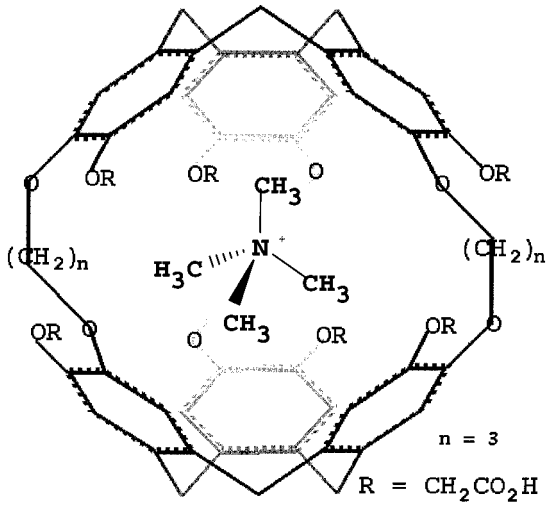

Figure 1. The structure of the cryptophane−TMA^+ host−guest system used in this study.

A representation of the cryptophane−TMA^+ complex used in this study is displayed in Figure 1. The cryptophane is a hexa-acid derivative of cryptophane-E, and its binding properties for ammonium guests including TMA^+ have recently been reported.[22] The cryptophane contains two cyclotriveratrylene groups, each comprising three aromatic rings connected by methylene bridges. Each aromatic ring is bonded to an acetic acid group through an ether linkage. The two cyclotriveratrylene groups are joined together by three phenolic propyl linkers to form a roughly spherical molecule with a cavity. The propyl linkers along with the acetic acid groups form pores through which a guest must pass to bind with the cryptophane.

Methods

Consistency with Previous Study. Every effort has been made to keep the current study as consistent as possible with the previous one. Where applicable, the same atomic, system, equilibration, and molecular dynamics parameters have been used as in the previous study. For completeness, the methods used in this study will be outlined here; many of the details can be found in the previous paper.[21]

Atomic Parameters. An all-atom representation was employed for both the cryptophane and TMA^+ molecules in this system. Internal bonded parameters were obtained from the AMBER parametrization.[23] Nonbonded parameters were obtained from two sources. The Lennard-Jones parameters were obtained from the OPLS parametrization with all-atom extensions.[24,25] All 1−4 interactions not involving polar−polar interactions have been scaled by $^1/_8$. The 1−4 polar−polar interactions, namely the 1−4 acid oxygen to ether oxygen interactions, have been scaled by $^1/_2$, as discussed before.[21]

The same atomic charges used for the cryptophane molecule in the previous study were used in the current one. These atomic charges were derived by dividing the cryptophane molecule into 15 fragments. Four unique fragments identified as ACET, ACID, ARYL, and PRPL resulted from these divisions. Auxiliary groups were added at the division points to form four complete molecules. Atomic centered charges were then derived by conducting ab initio calculations on each of the resulting molecules individually. The details are left to the previous paper.[21]

Table 1. Nonbonded Parameters Used for TMA^+

OPLS atom type	ϵ (kcal/mol)	σ (Å)	charge
101 N3	0.170	3.25	0.208
291 CT	0.066	3.50	−0.270
295 HC	0.030	2.50	0.156

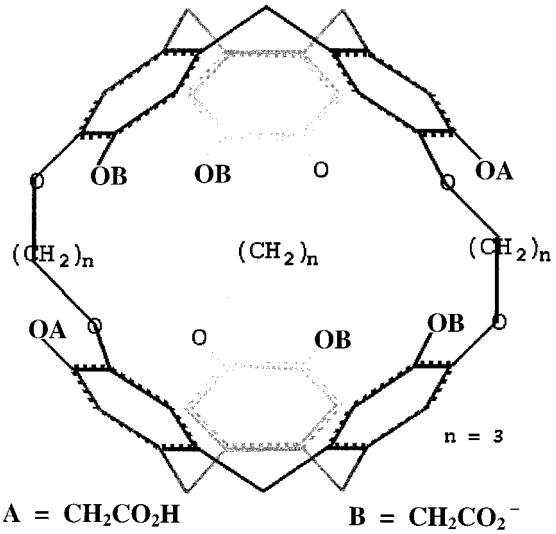

Figure 2. Arrangement of the ACET and ACID groups on the cryptophane molecule. The TMA^+ molecule is not shown.

TMA^+ atomic charges were determined in a similar fashion, but because of its size did not require division into fragments and addition of auxiliary groups. Table 1 lists the atom types, Lennard-Jones parameters, and atomic charges used for the TMA^+ molecule in this study. These TMA^+ charges are similar to what others have used for TMA^+.[26] Nonbonded parameters used for the cryptophane molecule are tabulated in ref 21. In this study and in the previous, all 1−4 Coulombic interactions were scaled by $^1/_2$.

Molecular System. For solubility reasons, experimental studies conducted in water involve the cryptophane molecule titrated until four of the six acetic acid groups are ionized.[22] Likewise, in this and in the previous computational study, the cryptophane molecule was modeled with four of its acid protons removed, giving the complex an overall charge of −3 (−4 for cryptophane, +1 for TMA^+). The protons were removed as illustrated in Figure 2, resulting in one of the cryptophane pores containing an ACET/ACET pair and the other two pores containing ACET/ACID pairs (TMA^+ not shown).

To form the host−guest complex, TMA^+ coordinates were built into cryptophane coordinates taken from the previous study. The model was immersed in a cubic periodic box of SPC/E water[27] with dimensions of 35 × 35 × 35 Å. Water molecules whose oxygens were within 2.0 Å of a heavy atom of the cryptophane or TMA^+ were removed. As a result the system contained 1384 SPC/E water molecules. (The previous study involved 1387 SPC/E water molecules.)

Molecular dynamics simulations were conducted on the system with use of ARGOS V7.0.[28] In all calculations, a 14.0-Å long-range nonbonded cutoff (forces evaluated once every 10 steps) and a 9.0-Å short-range nonbonded cutoff (forces evaluated every step) to the energy expression were used. The nonbonded pair list was evaluated every 10 steps. By using a 14.0-Å cutoff, all intramolecular nonbonded interactions were included. Use of an Ewald or other method to eliminate cutoffs entirely would be desirable, but would not be expected to alter the results presented here substantially because the host and guest molecules are fairly symmetrical and a rather large value is used for the long-range cutoff. SHAKE was used to fix all bond lengths to their equilibrium values.[29]

(21) Kirchhoff, P. D.; Bass, M. B.; Hanks, B. A.; Briggs, J. M.; Collet, A.; McCammon, J.A. *J. Am. Chem. Soc.* **1996**, *118*, 3237−3246.
(22) Garel, L.; Lozach, B.; Dutasta, J.-P.; Collet, A. *J. Am. Chem. Soc.* **1993**, *115*, 11652−11653.
(23) Weiner, S. J.; Kollman, P. A.; Nguyen, D. T.; Case, D. A. *J. Comput. Chem.* **1986**, *7*, 230−252.
(24) Jorgensen, W. L.; Tirado-Rivers, J. *J. Am. Chem. Soc.* **1988**, *110*, 1657−1666.
(25) Jorgensen, W. L.; Severance, D. L. *J. Am. Chem. Soc.* **1990**, *112*, 4768−4774.
(26) Personal communications with T. P. Straatsma and Erik Hom.
(27) Berendsen, H. J. C.; Grigera, J. R.; Straatsma, T. P. *J. Phys. Chem.* **1987**, *91*, 6269−6271.
(28) Straatsma, T. P.; McCammon, J. A. *J. Comput. Chem.* **1990**, *11*, 943−951.

Equilibration of the System. Equilibration of the system was conducted by first relaxing the solvent energy with steepest decent while the solute was held fixed. Second, molecular dynamics was conducted on the solvent at 298 K for 20 ps with velocity reassignment every 0.2 ps while the solute was held fixed. Third, molecular dynamics was conducted on the entire system for 5-ps intervals at temperatures of 100, 200, and 298 K with velocity reassignment every 0.2 ps. Finally, molecular dynamics was conducted on the entire system at 298 K for 10 ps with velocity reassignment every 0.5 ps followed by a 20-ps simulation with no velocity reassignment. During the equilibration, the short-range cutoff for solvent−solvent interactions was 7 Å through the 100 K run, 8 Å for the 200 K run, and 9 Å for the remainder of the equilibration. A time step of 2.0 fs was used in all equilibration molecular dynamics.

Molecular Dynamics Simulations. Molecular dynamics was performed at 298 K in the NPT ensemble. The temperature was maintained by weak coupling to a temperature bath by separate solute and solvent temperature scaling by using a 0.1-ps coupling constant. The pressure was maintained at 1.0×10^5 Pa, using a compressibility of 4.5×10^{-10} m^2/N and a pressure relaxation time constant of 0.5 ps. The time step during dynamics was 2.0 fs. An analysis run was conducted for 25 ns. Conformational analysis was conducted at every step, and pore and cavity calculations were conducted at every 0.1 ps.

Results and Discussion

General Structural Information. As in the case of the uncomplexed cryptophane, the cryptophane−TMA^+ complex remains roughly spherical throughout the entire simulation. The TMA^+ molecule, which remained within the cavity during the 25 ns of simulation, was able to rotate independently of the cryptophane molecule. Figure 3 displays stereoplots of the complex at 5-ns intervals. It has been suggested that the greater binding stability of TMA^+ with this cryptophane, as opposed to some larger guests, might be due to the ability of the TMA^+ molecule to rotate within the cavity.[22]

Water molecules within the cryptophane cavity would likely be displaced, at least in part, upon the binding of another guest. The presence of water molecules within or near the cryptophane cavity could, however, help stabilize a host−guest complex. Complete system configurations consisting of all cryptophane, TMA^+, and water atomic coordinates were analyzed at 25-ps intervals during the last 24 ns of simulation. Cavity radii excluding the presence of the TMA^+ molecule (calculated as described below) were used along with the system configurations to determine the number of water molecules within the cavity at each of these structures as well as the average number within the cavity. For each structure, its center of geometry based on the cap and linker regions (atoms making up the "ARYL" and "PRPL" fragments) was determined. A water molecule was considered to fall within the cryptophane's cavity if its oxygen atom lay within the cavity radius from the center of geometry. In the previous study involving the uncomplexed cryptophane, it was determined that the number of water molecules within the cavity ranged from 0 to 5, with an average number of 2.1. In the current study involving the cryptophane−TMA^+ complex, no water molecules were ever found within the cavity. These results suggest that water molecules are fully displaced from the cavity upon the binding of TMA^+ with this specific cryptophane, and that they do not contribute to the stability of the host−guest complex by, e.g., forming internal bridges between host and guest.

Because of their location, the ACET and ACID fragments play a role in the gating of the cryptophane pores. However, these fragments could also play an additional role in the stabilization of a complex, especially complexes involving charged guests. For this reason, it is of interest to examine the displacements of the ACET and ACID fragments, comparing the complexed to uncomplexed systems. Figure 4 displays histograms of the carboxylate carbon to the center of geometry distances. The center of geometry is based on the cap and linker regions of the host—atoms making up the "ARYL" and "PRPL" fragments. The histograms represent the percentage of structures in each bin for the total number of structures analyzed. For the complexed system, structures were analyzed at 0.1-ps intervals throughout the 25-ns simulation. For the uncomplexed system, structures were analyzed at 0.05-ps intervals throughout the 20-ns simulation. Plots for each of the ACET and ACID groups are shown for both the complexed and uncomplexed systems.

The most striking feature of these plots is the greater mobility and the closer approach to the center of geometry of the neutral ACID groups as compared to the charged ACET for both the complexed and uncomplexed systems. This makes sense in terms of solvation effects. The ACET groups, being charged, interact more strongly with the surrounding water than do the neutral ACID groups. Interaction with the surrounding water molecules tends to suppress the fluctuations of the ACET groups while keeping them extended away from the cryptophane cavity.

Comparing the plots for the complexed to the uncomplexed systems shows a number of other interesting features. For both fragments, but especially for the ACID groups, the presence of the TMA^+ molecule reduces their mobility and limits how closely they approach the cryptophane cavity. This is likely due simply to the presence of the relatively large single guest molecule (TMA^+) as opposed to several smaller guest molecules (water molecules) which are capable of moving independently of one another. Importantly, there is no significant collapse of the ACET groups toward the TMA^+ molecule in the complex as one might expect from a purely Coulombic anion−cation interaction. Again this makes sense in terms of solvation effects. The charge on the ACET groups can be stabilized by several polar water molecules as effectively as by a single large cation with a delocalized charge.

These results suggest that the stabilization of the cryptophane−TMA^+ complex is not due simply to cation−anion (TMA^+−ACET) interactions. This could be tested experimentally by determining the binding energy of TMA^+ to cryptophane after titrating the cryptophane with various equivalents of NaOH. The lack of a strong dependence on the binding energy with the number of ionized groups would support this view.

Conformational Analysis. Conformational analysis was conducted on the cryptophane molecule of the cryptophane−TMA^+ complex to make comparisons to the previous analysis of the uncomplexed system. As in the previous study, the rate at which unique conformations are being sampled with simulation time was computed by analyzing the cryptophane's dihedral angles. To do this, each angle was divided into wells. Divisions between wells occur at the maxima in the dihedral potential function for each angle. At each molecular dynamics step, every angle was assigned an integer designating which well the angle currently occupied. In this way, the conformation of the cryptophane at each molecular dynamics step was defined by a string of integer values. Included with the integer string was the molecular dynamics step at which it was created. Excluding the indistinguishability of certain atoms and symmetry considerations, two integer strings defined the same conformation only if they were identical.

Dihedral angles for the TMA^+ molecule were completely excluded from the analysis. Only dihedral angles for the

(29) Ryckaert, J. P.; Ciccotti, G.; Berendesen, H. J. C. *J. Comput. Phys.* **1977**, *23*, 327−341.

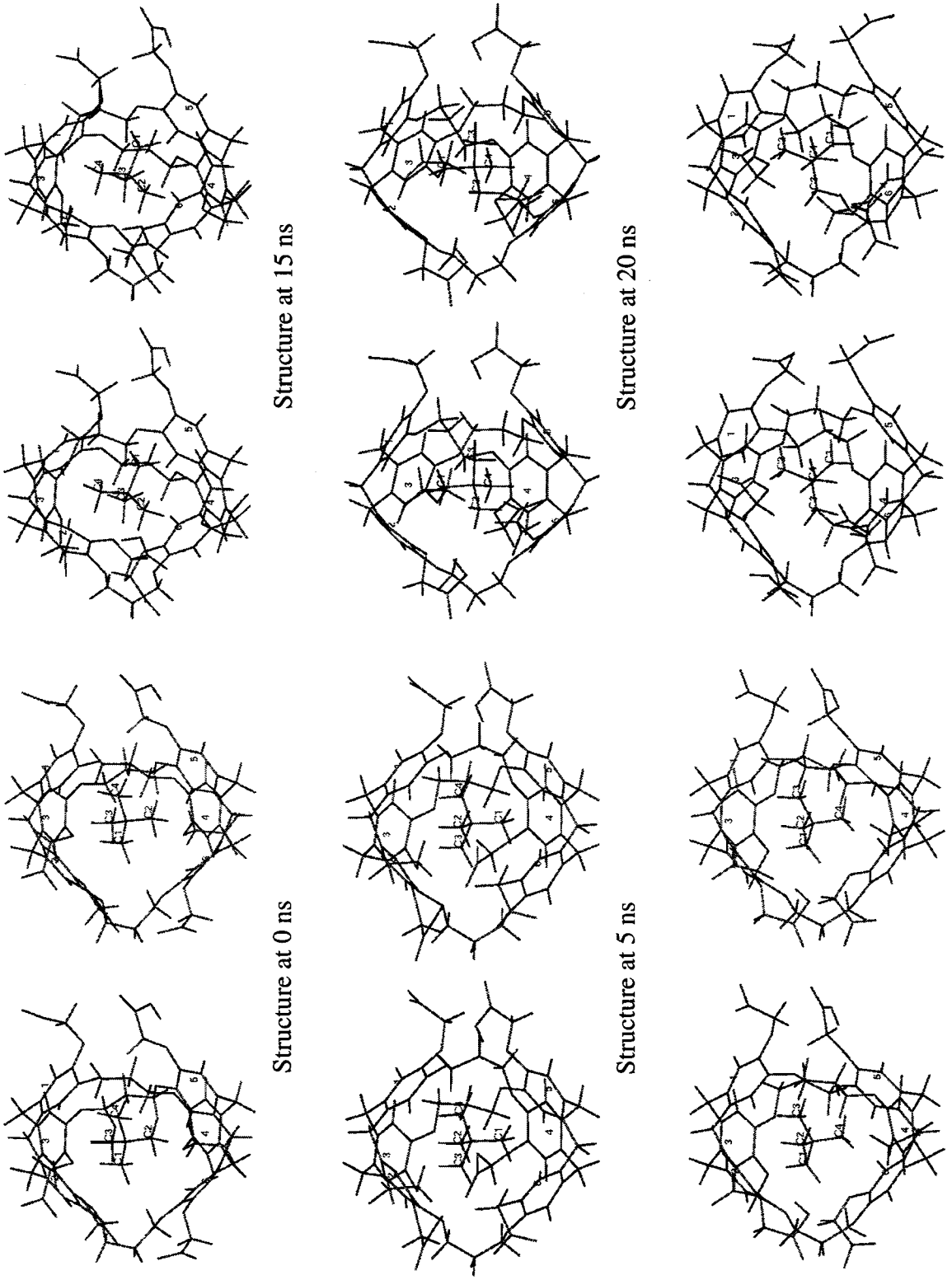

Figure 3. Stereoplots of the complex are displayed at 5-ns intervals. The structures are in approximately the same orientation with a number of the cryptophane and TMA^+ atoms labeled by atom and residue number to illustrate the independent rotation of the two molecules.

Table 2. Results of Conformational Analysis

	host 20 ns		host−guest 20 ns		host−guest 25 ns	
region	# sampled unique	# sampled unique − equivalent	# sampled unique	# sampled unique − equivalent	# sampled unique	# sampled unique − equivalent
whole	890 042	889 624	180 372	176 739	230 585	223 940
exo	154 868		117 557		146 245	
cage	49 280	29 749	1 439	1 024	1 615	1 130

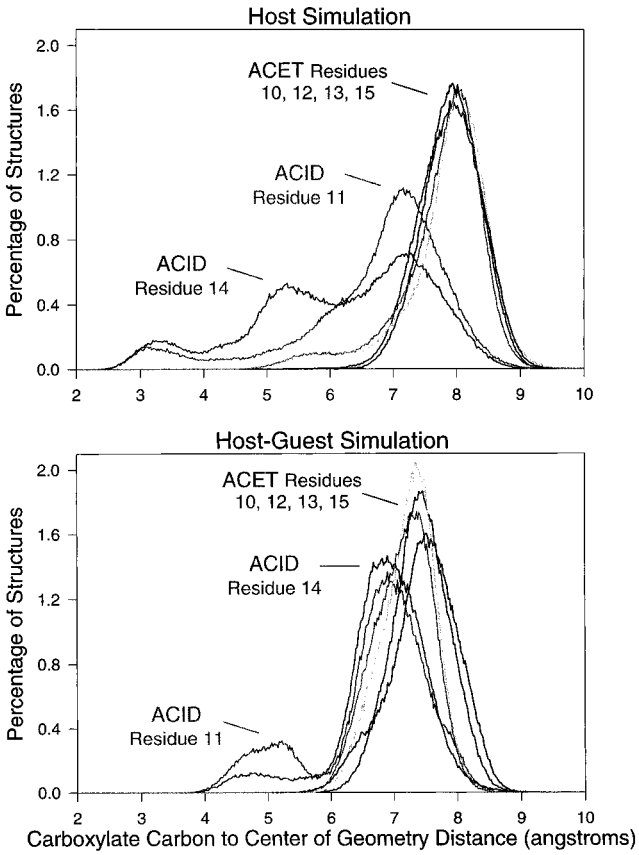

Figure 4. Histograms of the carboxylate carbon to the center of geometry distances. The histograms represent the percentage of structures in each bin for the total number of structures analyzed. The same bin size was used for each of the plots.

cryptophane molecule were analyzed. Of the 412 proper and improper dihedral angles making up the cryptophane molecule, only the 54 angles used in the previous study were used in this study. The other 358 angles either did not undergo rotameric transitions during the course of the simulation and therefore did not contribute to the formation of unique conformations or involved protons and were excluded to simplify the analysis.

To determine the rate at which unique conformations were being sampled with simulation time, the conformational analysis was conducted in a top-down fashion. Starting at the beginning of the simulation, unique conformations and the simulation time in which they were generated were saved. Conformations which were not unique, having been sampled earlier in the simulation, were removed. The result was a list of unique conformations and the time in which they were first sampled.

In addition to conducting conformational analysis on the "whole" cryptophane, conformational analysis was also conducted separately on two regions of the cryptophane. The "exo" region was defined as consisting of the ACID and ACET groups up through and including the ether oxygens. The remainder of the cryptophane was defined as the "cage" region. The fluctuations of the cage region may be particularly relevant to the binding of guest molecules such as TMA$^+$. The number of conformations sampled in the whole, cage, and exo regions for the complexed and uncomplexed cryptophane are listed in Table 2. To make a direct comparison to the previous study possible, the number of conformations sampled for the complex up to just 20 ns of simulation is also listed.

One would expect that the presence of one large guest within the cavity as opposed to several smaller guests would make the cryptophane molecule, and especially its cage region, more rigid. The increased rigidity would be expected to decrease the rate at which unique conformations were sampled. (It might also result in a decrease of the total number of conformations available to the cryptophane on an energetic basis, but this cannot be determined without comprehensive sampling.) This is exactly what is observed. The complexed cryptophane molecule sampled fewer unique conformations than the uncomplexed molecule. The cage region showed the largest decrease in the sampling of unique conformations of about 34 times in the 20-ns period. The exo region showed a decrease of only about 1.3 times, and the whole molecule showed a decrease of about 4.9 times.

As in the previous study, the equivalence of the generated structures was also considered. Two structures were considered equivalent if the molecule could be rotated so that the corresponding rotameric states were the same. The results for the number of unique conformations sampled for the cryptophane and the cage region with the equivalent conformations removed are also displayed in Table 2. With the equivalent structures removed, the cage region showed a decrease in the sampling of about 29 times in the 20-ns period, the whole molecule showing a decrease of about 5.0 times. Assuming that the converged number of distinct conformations available to the host molecule is reduced by a factor of 5 on binding of TMA$^+$, and that these conformations are of similar energy, binding of the guest would result in an unfavorable change in the entropy of $\Delta S_{conf} = R \ln(1/5)$, corresponding to a $\Delta G_{conf} \approx 1$ kcal/mol at $T = 300$ K.

Plots of unique conformations sampled with simulation time for the whole cryptophane and the cage region are displayed in Figure 5. For the whole cryptophane, unique conformations were rapidly sampled throughout the entire simulation. The cage region, however, shows a series of plateaus in the sampling followed by bursts of new conformations.

Pore and Cavity Calculations. Pore and cavity radii were determined for the cryptophane molecule of the complex excluding the presence of the TMA$^+$ molecule. The analysis was conducted every 0.1 ps throughout the 25-ns simulation. (In the previous study of the uncomplexed cryptophane, the analysis was conducted every 0.05 ps throughout the 20 ns of simulation.) The radii were determined to further describe the structural character of the complex and to gain an indication of how the presence of the guest affects pore fluctuations and possibly binding and release rates. This analysis also provided a means to determine an effective radius for the TMA$^+$ molecule for comparisons with the calculated pore and cavity radii.

As in the earlier study, pore and cavity radii were obtained for each cryptophane structure analyzed by generating a series of probe-accessible dot surfaces, such as that of Lee and

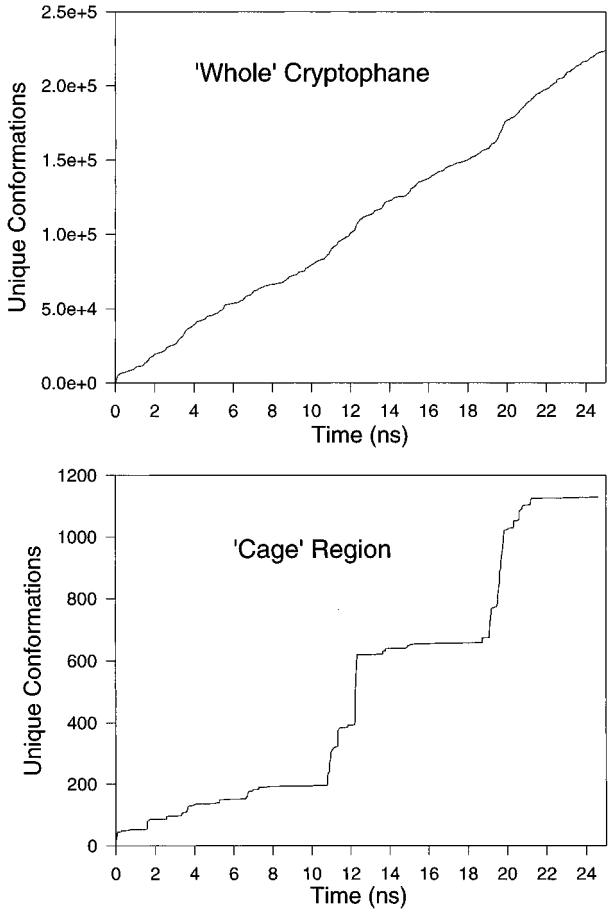

Figure 5. Unique conformations sampled with simulation time for the whole cryptophane and the cage region. Equivalent structures have been removed.

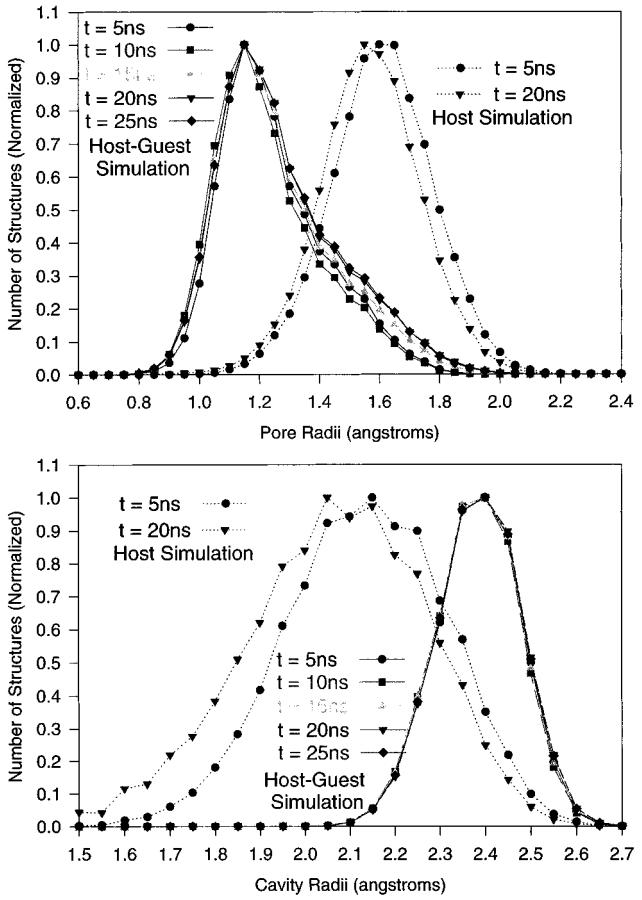

Figure 6. Convergence of pore and cavity radii with simulation time for both the host and host−guest systems. The plots represent distributions of radii at increasing durations of simulation time. Each plot has been normalized to its maximum bin value.

Richards,[30] using a series of probe radii. The method used and the type of analysis described below are similar to those used in a recent study of structural fluctuations in an enzyme that may allow substrate to penetrate to, and products to escape from, a buried active site.[31] The surfaces were generated by using an all-atom representation with atomic radii based on one-half the OPLS Lennard-Jones σ values used in the molecular dynamics simulation. The actual values used for the atomic radii in the surface generation were 1.81 (carbon), 1.50 (oxygen), and 1.25 Å (hydrogen). All TMA^+ atoms and all water molecules were excluded from these calculations. Only the coordinates of the cryptophane were used.

The probe-accessible dot surface for a given probe radius was then generated by evenly distributing 182 "sphere" points around the center of each atom at a distance of the atomic radius plus the probe radius for that surface. To create the surface, every sphere point of every atom was checked to see if it lay within a distance of the atomic radius plus the probe radius of any other atom in the cryptophane. Sphere points which did lie within this distance were eliminated. The remaining sphere points made up the surface, which could consist of one continuous surface or a number of discrete surface clusters.

For each probe-accessible dot surface generated, the number of discrete clusters of surface points was determined. A cluster of points was considered discrete if the points were separated from other points outside the cluster by a distance relative to the spacing of the 182 sphere points. The value used for this distance was twice the greatest distance between any sphere point and its nearest neighbor for points distributed on a sphere with a radius equal to the carbon atomic radius plus the probe radius used in the generation of that surface.

The pore and cavity radii for a given cryptophane−TMA^+ structure were then determined by following the formation of discrete clusters of surface points as the probe radius was varied. The pore radius was determined by increasing the probe radius incrementally until two discrete clusters of surface points were formed, one cluster of surface points forming the outer surface of the cryptophane, the other cluster forming the internal cavity surface. This radius defines the maximum size of a probe that can enter into the cavity for a given structure of the cryptophane. No differentiation was made between the three pores. Only the radius for the largest pore of each cryptophane structure was determined. As the probe radius was further increased, a point was reached where the internal cavity surface no longer had surface points. This radius defined the size of the internal cavity for a given structure of the cryptophane.[32]

The calculated distributions of pore and cavity radii converged within about 5 ns of simulation. Figure 6 displays normalized pore and cavity radii distributions at increasing durations of simulation time for both the complexed and uncomplexed cryptophane. For the structures sampled in the course of the 25-ns simulation, the complexed cryptophane had an average pore radius of 1.27 Å, a minimum of 0.61 Å, and a maximum

(30) Lee, B.; Richards, F. M. *J. Mol. Biol.* **1971**, *55*, 379−400.

(31) Gilson, M. K.; Straatsma, T. P.; McCammon, J. A.; Ripoll, D. R.; Faerman, C. H.; Axelsen, P. H.; Silman, I.; Sussman, J. L. *Science* **1994**, *263*, 1276−1278.

(32) For very small probe radii, especially in the all-atom representation, discrete clusters of surface points can form which do not represent the outer and cavity surfaces. Therefore as a matter of practice, calculations were started with a large probe radius which was incrementally decreased to determine the cavity then the pore radius for a given cryptophane structure.

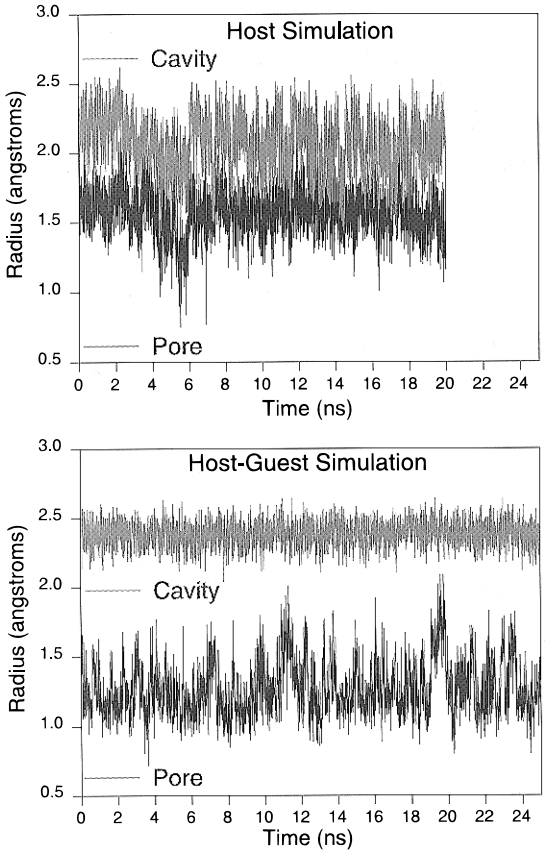

Figure 7. Pore and cavity radii as a function of simulation time for both the host and host−guest systems. Data are plotted at 5-ps intervals throughout each simulation. Mean, minimum, and maximum values for the radii reported in the text are based on all structures analyzed.

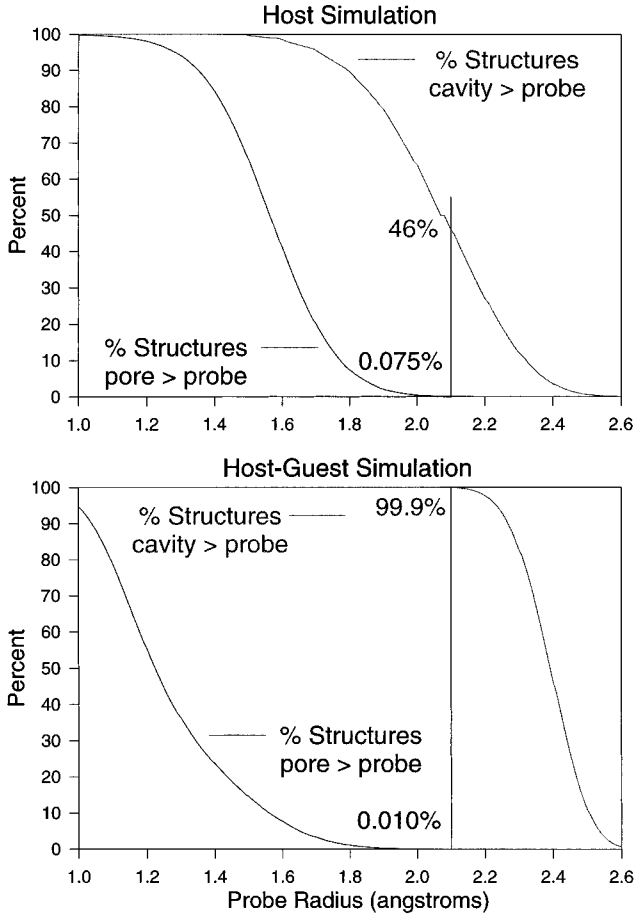

Figure 8. Percentage plots of structures whose pore and cavity radii are greater than a probe radius. The vertical line is drawn at a probe radius of 2.10 Å, which is the effective radius for the TMA$^+$ molecule. The percentages of structures with pore and cavity radii greater than the probe radius of 2.10 Å is indicated on the graph.

of 2.22 Å. The cavity had an average radius of 2.38 Å, a minimum of 1.95 Å, and a maximum of 2.75 Å. (The uncomplexed cryptophane pore had mean, minimum, and maximum values of 1.57, 0.59, and 2.46 Å, respectively, and cavity radii with mean, minimum, and maximum values of 2.07, 1.40, and 2.74 Å, respectively.) Figure 7 displays plots of pore and cavity radii as a function of simulation time for both the complexed and uncomplexed cryptophane molecules. The data are plotted at 5-ps intervals.

Figures 6 and 7 illustrate how the presence of the TMA$^+$ guest affects the fluctuations of the cryptophane molecule. The guest causes the cryptophane's cage to stretch, which results in a larger average cavity radius and a decrease in the fluctuations of the cavity radii. The stretching of the cage restricts the movements of the PRPL groups, which in turn decreases the average pore radius. This restriction does not, however, prevent an occasional large fluctuation in the pore radius as can be seen in both of these figures. This is due to the fact that the ACET and ACID groups are not greatly affected by the presence of the guest.

To gain a rough indication of the ease with which a cryptophane could contain a guest within its cavity or allow a guest molecule to pass through its pores, plots of the percentages of structures whose pore and cavity radii are greater than a probe radius were generated. These plots are displayed in Figure 8 for both the complexed and uncomplexed cryptophane. A vertical line is drawn on each graph at a probe radius of 2.10 Å, which was considered the effective radius of a TMA$^+$. The effective radius of TMA$^+$ used here was defined as the distance between the nitrogen at the geometric center of the molecule and one of the methyl protons. This radius is smaller than the largest distance from the nitrogen to the van der Waals surface of the molecule, reflecting the fact that the aspherical guest will tend to present less than its maximum cross section as it enters a pore.

These plots indicate that the use of 2.10 Å as an effective radius for TMA$^+$ is a reasonable choice for comparison with the calculated pore and cavity radii as determined in these studies. The minimum radius obtained for the cavity with the TMA$^+$ molecule present was 1.95 Å, and 99.9% of the cryptophane structures had a cavity radius of greater than 2.10 Å. Notice also from these plots that the number of pores large enough to admit or release a guest of 2.10 Å radius drops from 0.075% to 0.010%. This suggests that the binding of a TMA$^+$ molecule might be easier than the release of a TMA$^+$ molecule that is already bound.

Stochastic Gating. The steady-state binding rate of TMA$^+$ and other guests which bind within the cavity would presumably be nearly diffusion limited if it were not for the fact that the guest must pass through a fluctuating pore to reach the cavity of the cryptophane. As in the previous study, the effect of the cryptophane pore fluctuations on binding rate of a particular guest was analyzed qualitatively as a stochastically gated reaction. The relevant process in this case is the exchange of a TMA$^+$ that is already bound by a guest from the solution. There are two limiting cases for a diffusion-influenced, stochastically gated reaction.[33]

In one limiting case, the opening and closing of the gate (e.g. the fluctuation of the pore radii) is slow compared to the

(33) Szabo, A.; Shoup, D.; Northrup, S. H.; McCammon, J. A. *J. Chem. Phys.* **1982**, *77*(9), 4484−4493.

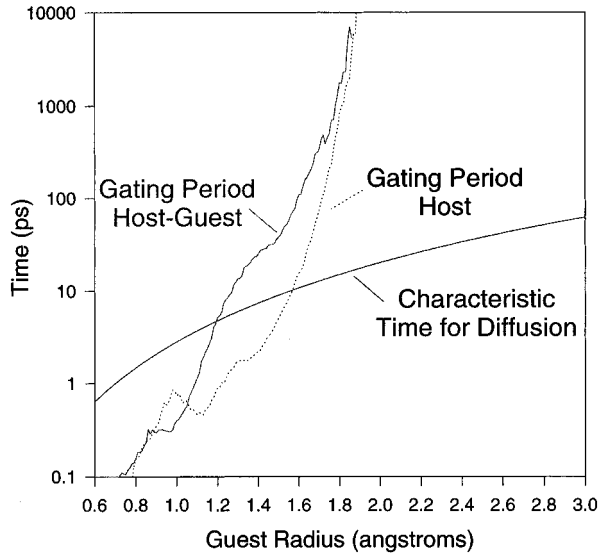

Figure 9. Influence of pore fluctuations on binding kinetics as a function of guest radius.

characteristic time for diffusion of the cryptophane and the guest. In this case (Case I), the overall rate constant is the steady-state association rate constant for the reaction with the gate fixed open, multiplied by the equilibrium probability that the gate is open. In the other limiting case (Case II), the opening and closing of the gate is fast compared to the characteristic time for diffusion of the cryptophane and the guest. In this case the overall rate constant is simply the steady-state association rate constant for the system with the gate fixed open. This is due to the fact that the gate is very likely to open during any diffusional encounter. For the system considered here, the above cases both assume that the initially-bound guest dissociates readily when the gate is open, so that a new guest can bind.

To gain insight into how the size of a guest and its presence within the cavity would affect binding, the characteristic time for diffusion of the cryptophane and guest was compared to a gating period defined for the cryptophane based on the fluctuations of its pore radii. As before the analysis here is qualitative. A more detailed analysis based on the theory of ref 33 does not seem warranted in view of the approximations made for the parameters of the theory as applied here.

Both the characteristic time for diffusion and the gating period are functions of the host and guest size. These functions are displayed in Figure 9 for the complexed and uncomplexed cryptophane. For these calculations the host was considered to be spherical with a constant radius. Radius values of 7.61 and 7.84 Å were used for the complexed and uncomplexed cryptophane, respectively. These values correspond to the average radius of the cryptophane defined as the average distance between the center of geometry of the cryptophane and the carboxylate oxygen atoms. The average radius was obtained from cryptophane structures saved at 5-ps intervals throughout each simulation.

Because of the difference in radii, the characteristic time for diffusion differs between the complexed and uncomplexed systems. This difference, however, is not enough to be visible on the graph. In generating the gating periods for the two systems, the difference in sampling frequency of the complexed and uncomplexed cryptophane was taken into account. Structures were sampled every 0.1 ps for the complexed and 0.05 ps for the uncomplexed cryptophane. All other parameters, definitions, and equations used are exactly the same as in the previous study. These details are reported in ref 21.

As can be seen in Figure 9, values for the gating period and the characteristic time for diffusion intersect at guest radii of approximately 1.2 and 1.6 Å for the complexed and uncomplexed systems. In the regions of intersection, the gating periods for the complexed and for the uncomplexed cryptophane are both rapidly increasing relative to the characteristic time for diffusion. Therefore, for the complexed cryptophane, guests with atomic radii larger than 1.2 Å will tend toward Case I of a diffusion-influenced, stochastically gated reaction. That is, the overall rate constant for the binding of the guest within the cryptophane will be the steady-state association rate constant for binding of the guest with the cryptophane pores fixed open, multiplied by the equilibrium probability that the pores are open. The pore size and fluctuations affect the binding rates of guests with radii larger than 1.2 Å.

Guests with atomic radii smaller than 1.2 Å will tend toward Case II of a diffusion-influenced, stochastically gated reaction. That is, the overall rate constant for the binding of the guest within the cryptophane will be the steady-state association rate constant for binding of the guest with the cryptophane pores fixed open. The pore size and fluctuations do not affect the binding rates of guests with radii smaller than 1.2 Å, except for the possible indirect effect of slow release of the previously-bound TMA^+.

Concluding Remarks

The presence of the TMA^+ molecule within the cavity causes the cryptophane to stretch and the cage region to become more rigid. As a result, fluctuations allowing for open events in which a TMA^+ molecule may pass through a pore are less likely in the complexed versus the uncomplexed systems. This leads to the notion that a guest molecule may tend to remain within the cavity for kinetic reasons. That is, the presence of the guest may slow the fluctuations necessary for its release, leading to longer lifetimes of the complex.

Such a notion may apply to some biological systems. It is often observed that active sites are located deep within an enzyme such as in the case of acetylcholinesterase (AChE). There are many reasons why an active site might need to be buried or contained within a pocket as opposed to being on the surface of an enzyme. Such reasons may include the need for a special environment for the reaction to occur, the need to separate reactants or intermediates from the surrounding solution to prevent side reactions, etc. Another reason why it may be advantageous to enclose an active site in some cases may be the need to kinetically trap the reactants, while possibly allowing for the relatively easy release of products. For example, an enzyme whose function is to hydrolyze a single reactant molecule into two or more smaller products could improve its overall turnover in a nonequilibrium situation if the reactant molecule is kinetically trapped within the active site but the smaller product molecules are not.

Acknowledgment. The authors would like to thank Dr. T. P. Straatsma for the use of ARGOS, Dr. Michael Gilson for providing the surfacing code adapted for use in the pore and cavity determinations and for his advice, and Dr. Michael Bass for providing the TMA^+ atomic charges. P.D.K. thanks Dr. Adrian Elcock, Dr. Tami Marrone, and Michael Potter and other members of the McCammon group for their suggestions, comments, and support of this study. This work was supported in part by grants from NSF and the NSF Supercomputer Centers MetaCenter Program.

JA971186D